Catalysis Communications 114 (2018) 79–83

Contents lists available at ScienceDirect

Catalysis Communications

journal homepage: www.elsevier.com/locate/catcom

Short communication

Strong affinity of mineral dusts for sulfur dioxide and catalytic mechanisms towards acid rain formation

Jiena Yun, Chang Zhu, Qian Wang, Qiaoli Hu, Gang Yang*

College of Resources and Environment, Chongqing Key Laboratory of Soil Multi-scale Interfacial Process, Southwest University, Chongqing 400715, China

ARTICLE INFO

Keywords:
Sulfur dioxide
Acid rain
Mineral dust
Catalytic mechanism
Density functional theory calculations

ABSTRACT

Mineral dust is an important arena for acid rain formation. Here, p-DFT calculations were conducted to study SO_2 adsorption onto gibbsite and possible catalytic mechanisms for acid rain formation. The obtained results clearly indicated that SO_2 is preferentially adsorbed onto mineral dusts instead of staying in the gas phase, and two catalytic paths were then posed. Path A with first hydrolysis and then oxidation is kinetically preferred, where SO_2 hydrolysis appeared to be the rate-determining step for all the investigated surfaces. Partially dehydrated gibbsite (100) surface has the lowest reaction barrier, and a second water molecule causes acid rain formation to occur facilely at ambient circumstances.

1. Introduction

Sulfur dioxide (SO_2) is one of the major precursors of acid rain that causes the acidification of soils and waters and accelerates the corrosion of buildings and monuments [1, 2]. Owing to the adverse impacts on the environment and human health, SO_2 emissions have recently grown into a global concern. Mineral dusts are the main components of haze and can be suspended in the air for a long time, allowing a plethora of atmospheric reactions to occur on their surfaces [3, 4]. Uptake of SO_2 by mineral dusts following with oxidation by ozone was suggested to be a viable route for sulfate formation [4], while a molecular-level understanding remains enigmatic.

The gas-phase hydrolysis of SO_2 and SO_3 has been widely investigated [5–13]. Liu et al. [7, 9] demonstrated that SO_2 hydrolysis in pure water clusters is thermodynamically unfavorable, and addition of ammonia or sulfuric acid reduces the reaction barrier substantially. Hazra and Sinha [12] showed that SO_3···H_2O···H_2O is the prevailing path for water to assist SO_3 hydrolysis, and formic acid (FA) leads to a similar complex (SO_3···H_2O···FA), while it causes the production of sulfuric acid (H_2SO_4) to be almost barrierless. To the best of our knowledge, the complete reaction mechanism from SO_2 to sulfuric acid (H_2SO_4) has scarcely been reported.

It was implicated that SO_2 can be taken up by mineral dusts [4], and in most regions, the high mass fraction of mineral dusts (10% to 20%) is a distinct feature of $PM_{2.5}$ [13]. Gibbsite, one of the most abundant secondary minerals on the Earth's surface, is the choice for this study, and periodic density functional theory (p-DFT) calculations were conducted to tackle the adsorption of SO_2 on gibbsite surfaces and the catalytic mechanism for SO_2 conversion to acid rain. In addition to regular surfaces, the partially dehydrated forms of gibbsite were taken into consideration because mineral dusts can also be presented in the dry state [14, 15]. It clearly indicated that gibbsite, especially when dehydrated, exhibits strong affinity for SO_2 as the metallic oxides of CuO and MgO reported previously [16–19] and hence should be an important arena for acid rain formation. The obtained results provide a molecular-level understanding for the production of acid rain over mineral dusts, and their critical role during acid rain formation has been disclosed.

2. Computational details

Atomic coordinates of gibbsite were taken from the crystalline structure reported by Saalfeld et al. [20] that is composed by the stacked sheets of linked octahedrons of aluminum hydroxide [21, 22]. Periodic models of regular (100) and (001) surfaces were composed by two unit cells (1 × 2 × 1), and a vacuum slab of 20.0 Å was built as shown in Fig. 1. The (100) and (001) surfaces of gibbsite were prepared experimentally and have been widely used in previous studies [23–25]. The surface energies (γ) can be estimated by the following Eq. (1):

$$\gamma = (E_{surf} - N*E_{bulk})/(2*A) \quad (1)$$

where E_{surf} and A stand for the electronic energy and surface area of gibbsite model, respectively. N refers to the number of the $Al(OH)_3$ formula units included in the gibbsite model, and the electronic energy of the $Al(OH)_3$ formula unit (E_{bulk}) was derived from bulk gibbsite.

The corresponding partially dehydrated surfaces of gibbsite were

* Corresponding author.
E-mail address: theobiochem@gmail.com (G. Yang).

https://doi.org/10.1016/j.catcom.2018.06.011
Received 20 February 2018; Received in revised form 11 June 2018; Accepted 13 June 2018
Available online 15 June 2018
1566-7367/ © 2018 Elsevier B.V. All rights reserved.

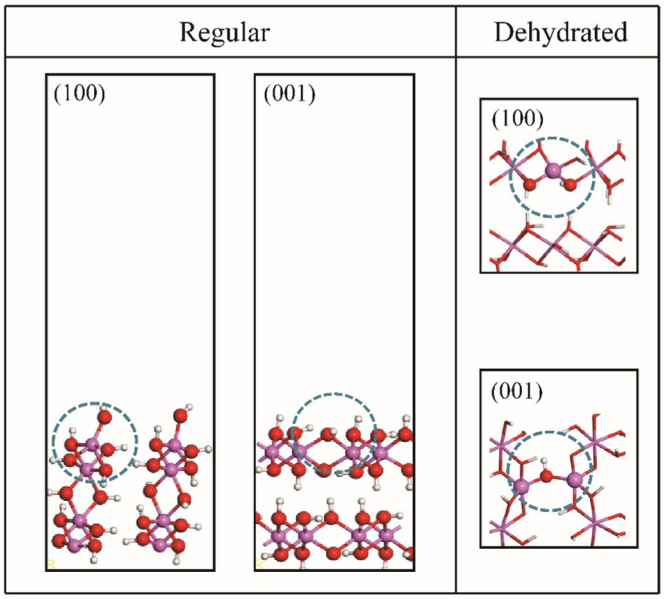

Fig. 1. Periodic models for (100) and (001) surfaces of gibbsite as well as local structures for the corresponding partially dehydrated surfaces.
Al, O and H atoms are in pink, red and white, respectively. The Al sites to construct the partially dehydrated surfaces are highlighted in blue dashed circles. (For interpretation of the references to colour in this figure legend, the reader is referred to the web version of this article.)

formed by removing one surface water molecule (Fig. 1), similar to the treatments for the partially dehydrated surfaces of goethite [17].

Periodic density functional theory (p-DFT) calculations with the generalized gradient approximation (GGA) were conducted using the Vienna Ab Initio Simulations Package (VASP) [26, 27]. The Perdew, Burke and Ernzerhof (PBE) [28] exchange-correlation functional was employed, and electron-ion interactions were handled by the projector augmented wave (PAW) method [29]. The dispersion interactions were accounted for by means of DFT + D2 approach. The energy cutoff was set to 400.0 eV. The Brillouin zone sampling was restricted to Γ-point, which has been verified to achieve the consistent structural and spectral results with experimental techniques and widely used in previous theoretical studies [18, 30–32].

3. Results and discussion

3.1. Adsorption of SO_2

The surface energies (γ) of the regular (001) and (100) surfaces of gibbsite are respectively calculated to be 0.4 and 0.2 $J{\cdot}m^{-2}$. Both values are very small and accordingly the formation of these two surfaces is energetically favorable [23–25]. Fig. 2 depicts the adsorption configurations of SO_2 onto the gibbsite (100) and (001) surfaces. All Al sites in regular (001) surface are six-fold and SO_2 interacts with the surface mainly through the O_{surf} atoms ("surf" in the subscript form refers to atoms from gibbsite surfaces), and the S-O_{surf} bond in **R1** is optimized at 2.374 Å. A structurally resembling adsorption configuration is detected for regular (100) surface; i.e., **R3**, where the S-O_{surf} bond equals 2.314 Å and one H-bond (O···H_{surf}: 2.252 Å) forms meanwhile. Two other adsorption configurations (**R1** and **R2**) are attained for regular (100) surface that are closely associated with the five-fold Al sites. Both **R1** and **R2** are characterized by two direct bonds, whereas the bonding interactions in **R1** are obviously stronger as evidenced by the shorter bond distances (S-O_{surf}: 1.798 vs. 2.177 Å and O-Al_{surf}: 1.910 vs. 2.115 Å). The adsorption energies of SO_2 are calculated to be $-70.2\ kJ{\cdot}mol^{-1}$ for **R1** of regular (001) surface and − 112.0, −86.6 and − 82.9 $kJ{\cdot}mol^{-1}$ for **R1**, **R2** and **R3** of regular (100) surface, respectively, in line with structural analyses. In consequence, gibbsite, especially (100) surface, shows strong affinity for SO_2, in line with the results of CuO and MgO metal oxides previously reported [16–19]. Thus, it is suggested that SO_2 should be favorably adsorbed onto mineral dusts instead of staying in the gas phase.

Mineral dusts can also exist in the dry state [14, 15] and the partially dehydrated form of gibbsite is considered (Fig. 1). Owing to dehydration, the lower-coordinated Al sites than those of regular surfaces are created, which result in more diverse and stronger affinity for SO_2. Four adsorption configurations are produced for each of the partially dehydrated (100) and (001) surfaces (Fig. 2). For example, regarding the partially dehydrated (100) surface, only one O atom of SO_2 in **D1** forms direct bond with Al_{surf}, and all three atoms of SO_2 in **D3** make direct bonds with the surface, whereas a stable four-membered ring appears in **D4** due to the fact that two neighboring surface atoms (Al_{surf} and O_{surf}) participate in the formation of direct bonds with SO_2. **D2** and **D4** are the optimal adsorption configurations for the partially dehydrated (001) and (100) surfaces, and the corresponding adsorption energies amount to −180.1 and − 167.6 $kJ{\cdot}mol^{-1}$, respectively. In consequence, the partial dehydration of gibbsite enhances pronouncedly the affinity for SO_2 and the results corroborate that atmospheric SO_2 should be preferentially adsorbed onto mineral dusts instead of staying in the gaseous state.

3.2. Catalytic reactions over partially dehydrated (100) gibbsite surface

Mineral dusts provide a good arena for catalytic reactions [4, 33] and following adsorption, SO_2 at gibbsite surfaces can react with water and ozone (O_3) towards acid rain formation [4]. Disparate reaction paths have been posed, and those of the partially dehydrated gibbsite (100) surface are shown in Figs. 3 (path A) and 4 (path B) together with their potential energies. For path A, **II** (**D4**) is the structure of SO_2 adsorption, and following water adsorption (Step 2: **II** → **III**), hydrolysis of SO_2 takes place (Step 3: **III** → [**TS1**] → **IV**) and produces the bisulfite species (HSO_3^-). During this step, the water molecule gets closer to SO_2 and the S—O3 distances are optimized at 3.010, 1.826 and 1.641 Å in **III**, **TS1** and **IV**, respectively. Meanwhile, one proton is transferred from water to the O_{surf} atom and in **TS1** bonds directly with the O1 atom of SO_2 (H-O1: 1.009 Å). The energy barrier for Step 3 is calculated to be $108.2\ kJ{\cdot}mol^{-1}$. An alternative for this step is the formation of sulphurous acid (H_2SO_3, see Fig. S1a), which possesses an overwhelmingly higher electronic energy of $129.8\ kJ{\cdot}mol^{-1}$ than the bisulfite species (HSO_3^-) and hence is almost thermodynamically forbidden. Step 4 (**IV** → **V**) is the adsorption of ozone (O_3), and its adsorption energy equals $-42.3\ kJ{\cdot}mol^{-1}$, suggesting that the adsorption process occurs favorably. The next step (Step 5: **V** → [**TS2**] → **VI**) is the oxidation of the bisulfite species (HSO_3^-) producing the hydrogen sulfate species (HSO_4^-). The O4-O5 and S—O4 distances are respectively optimized at 1.323 and 2.685 Å in **V**, 1.600 and 2.123 Å in **TS2** and 3.223 and 1.447 Å in **VI**, implying the breaking of O4-O5 bond and the formation of S—O4 bond during this step. Finally, the hydrogen sulfate species (HSO_4^-) deprives one proton from gibbsite surface and desorbs in the form of sulfuric acid (H_2SO_4). The energy barrier for Step 5 is $41.2\ kJ{\cdot}mol^{-1}$ and is apparently less than that of Step 3. Accordingly, hydrolysis of SO_2 is the rate-determining step for path A.

Path B deems the oxidation of SO_2 firstly and hydrolysis subsequently, in an inverse sequence as path A. As indicated in Fig. 4, the energy barriers for the SO_2 oxidation (Step 3: **III** → [**TS1**] → **IV**) and SO_3 hydrolysis (Step 5: **V** → [**TS2**] → **VI**) are calculated to be 11.5 and $147.2\ kJ{\cdot}mol^{-1}$, respectively, with the production of hydrogen sulfate species (HSO_4^-) as in the condition of path A. Hydrolysis of adsorbed SO_3 (**V**) to sulfuric acid (H_2SO_4, see Fig. S1b) is strongly disfavored and significantly endothermic ($79.4\ kJ{\cdot}mol^{-1}$) instead of exothermic ($-89.6\ kJ{\cdot}mol^{-1}$) for the hydrogen sulfate species (HSO_4^-). In consequence, hydrolysis is the rate-limiting step for both path A and path B, and both paths result in the formation of hydrogen sulfate species

Download English Version:

https://daneshyari.com/en/article/6502897

Download Persian Version:

https://daneshyari.com/article/6502897

Daneshyari.com